

Oxidation and Decomposition Kinetics of Thiourea Oxides

Qingyu Gao,^{*,†} Bing Liu,[†] Lianhe Li,[†] and Jichang Wang^{*,†,‡}

College of Chemical Engineering, China University of Mining and Technology, Xuzhou, Jiangsu Province 221008, People's Republic of China, and Department of Chemistry and Biochemistry, University of Windsor, Ontario N9P 3P4, Canada

Received: June 23, 2006; In Final Form: October 11, 2006

In this report the decomposition and oxidation kinetics of thiourea dioxide and thiourea trioxide are investigated with a reversed-phase ion-pair high-performance liquid chromatography (HPLC) method. The HPLC method allows us to simultaneously determine and quantify several sulfur-containing reagents such as $(\text{NH}_2)_2\text{CSO}_2$, $(\text{NH}_2)_2\text{CSO}_3$, $(\text{NH}_2)_2\text{CO}$, and SO_3^{2-} (HSO_3^-). Experiments illustrate that the decomposition of thiourea oxides is a first-order reaction, in which the rate constants increase with the pH of the solution. Oxidations of thiourea oxides by hydrogen peroxide are first order with respect to both reagents within the studied pH range between 4.0 and 8.0. Oxidation rate constants are measured under different pH conditions, which show that increasing the pH of the reaction solution significantly accelerates the oxidation process.

1. Introduction

Oxidations of thiourea oxides have received considerable attention in the past 3 decades because of their broad applications.^{1–11} For example, thiourea oxides have been frequently employed in the synthesis of guanidines and their derivatives, in which reactions of thiourea oxides with amines are generally carried out in organic solvents while reactions with amino acids take place in aqueous solutions.^{4–8} In addition, thiourea oxides have also been used in wastewater treatment, wool bleaching, and reducing organosulfur compounds such as disulfides and sulfoxides.^{9–11} Besides their usage as starting reactants, thiourea dioxide (TUO_2) and thiourea trioxide (TUO_3) are also postulated as the intermediate products in the oxidation of thiourea (TU).^{2,12} The oxidation of TU has been found to exhibit various exotic nonlinear phenomena including both periodic and quasi-periodic oscillations and the coexistence of two stable steady states.^{13–16} Therefore, understanding the stability and oxidation kinetics of TUO_2 and TUO_3 is critical in the study of nonlinear behavior in thiourea-based chemical oscillators.

Oxidations of thiourea oxides by various oxidants such as bromine, iodine, and chlorite have been reported by Simoyi and his group.^{12,17,18} Their studies illustrate that one of the final oxidation products of thiourea oxides is sulfate ion. In addition, they found that TUO_2 was a better reducing reactant than TUO_3 and aging of thiourea trioxide solution had significant effects on the observed reaction kinetics. When iodine was used to oxidize TUO_3 , they found that a pH increase led to the increased rate of reaction between I_2 and TUO_3 .¹⁸ Despite that oxidations of thiourea oxides have been investigated extensively, quantitative characterizations on the time evolution of concentrations of sulfur-containing species are still largely missing. Indeed, most of the existing studies had been performed by following variations of the concentration of oxidants, in which the reducing reagents, thiourea oxides, were in excess.¹² Such a constrained

configuration is partially because mixtures of sulfur compounds cannot be conveniently quantified with a UV–vis spectroscopic method. For example, Svarovsky and co-workers reported the interference of dithionite on the absorption of TUO_2 at 270 nm during their investigation of TUO_2 decomposition in air-saturated alkaline solution.¹⁷ Makarov and co-workers pointed out that the UV maxima of sulfite and TUO_3 are so close to each other that it is difficult to use UV spectroscopy for quantifying TUO_3 during its decomposition.¹⁸

To overcome the difficulties encountered in the UV–vis spectroscopic investigation, in this study we employed a reversed-phase ion-pair high-performance liquid chromatography (HPLC) method to investigate the decomposition and oxidation kinetics of thiourea oxides.¹⁹ As is shown in the following, the employment of HPLC allowed us to simultaneously determine and quantify several sulfur-containing reagents including TUO_2 , TUO_3 , sulfite, and urea, etc. These experimental measurements demonstrate that the reaction between hydrogen peroxide and thiourea oxides is first order with respect to both reagents.

2. Experimental Procedures

The chromatographic system used in this study comprises a Model G1379A pump with four pistons (Agilent 1100), a Model 7725 injection-valve equipped with a 20.0 μL sample loop (Rneodyne), and a Model G1365B MWD UV detector. Two separation columns were used in this research, i.e., a Phenomenex Ginimi C18 separation column (5.0 μm , 4.6 \times 250.0 mm) for decomposition experiments and Zorbax Bonus RP (5.0 μm , 4.6 \times 250.0 mm) for oxidation reactions. The mobile phase was prepared by mixing methanol and 2.5 mM tetrabutylammonium hydroxide ((TBA)OH) solution according to a volumetric ratio of 5–95. The sampling volume was kept constant at 10 μL . Water used in this study was distilled and then deionized with a Milli-Q system. An ultrasonic bath was used for sample degassing. Throughout this study, the methanol–(TBA)OH mixture was flowed at 0.5 mL/min for decomposition and 1.0 mL/min for oxidation measurements. Concentrations of reagents were determined by the integration of their peak areas. The buffer solution was prepared by mixing 0.05 M H_3PO_4

* To whom correspondence should be addressed. Fax: 86-516-3995758 (Q.G.); 1-519-978 7093 (J.W.). E-mail: gaoqy@cumt.edu.cn (Q.G.); jwang@uwindsor.ca (J.W.).

[†] China University of Mining and Technology.

[‡] University of Windsor.

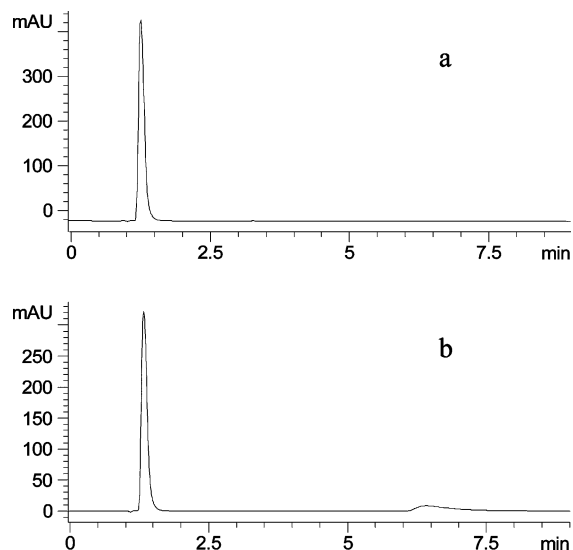


Figure 1. Chromatograms of the thiourea dioxide solution sampled at different times: (a) $t = 1.0$ min and (b) $t = 10080.0$ min. The solution is pH 3.0. The detection UV wavelength is 269.0 nm.

PO_4 and 0.05 M acetic acid solutions according to a 1:1 volumetric relationship and was then adjusted to the desired pH value with 2.0 M NaOH solution.

Hydrogen peroxide solution was titrated with a standard potassium permanganate solution. Formamidine sulfinic acid ($(\text{NH}_2)_2\text{SO}_2$, Fluka, >98%) was used without further purification. Formamidine sulfonic acid was prepared according to a synthetic procedure given in literature.^{7,18} The decomposition and oxidation reactions of thiourea oxides were conducted in a batch reactor thermostated through a circulating water bath (± 0.1 °C). All solutions were filtered through a 0.45 μm filter membrane and were degassed prior to use.

3. Results

To determine the concentration of each species through a chromatogram, it is necessary to establish the calibration curves that describe the relationship between the concentration and the area of each peak. The integrated areas of peaks representing TUO_2 and TUO_3 are found to possess excellent linear correlation with their concentrations, where the correlation coefficient is above 0.99 (see the Supporting Information). Concentrations of TUO_2 and TUO_3 in the following analysis are obtained by comparing the area of each peak with the calibration curves. Figure 1 characterizes the decomposition of thiourea dioxide in water, in which two chromatograms were collected respectively at (a) 1.0 and (b) 10 080.0 min. In this experiment, 0.04 g of TUO_2 was dissolved in 100.0 mL of water and the solution was adjusted to pH 3.0. The detection UV wavelength used in this measurement is 269 nm. As shown in the figure, the absorption peak of thiourea dioxide decreases significantly after 10 080.0 min. Meanwhile, a new peak with a resident time $t = 6.4$ min is detected. The newly formed species is confirmed to be HSO_3^- . Similar to oxygen-free decomposition of hydroxymethanesulfinic acid,²⁰ HSO_3^- could be produced through the following steps:

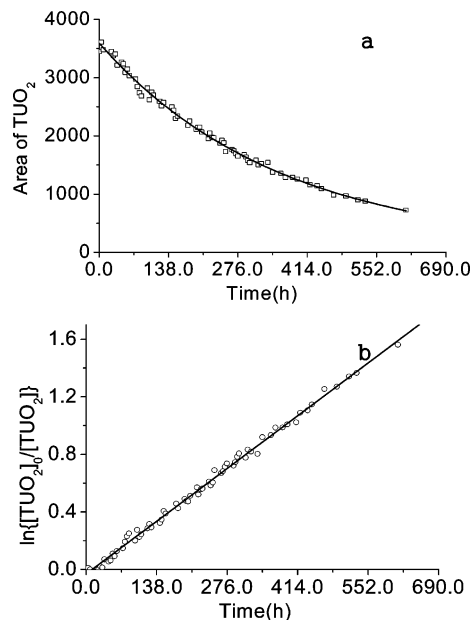
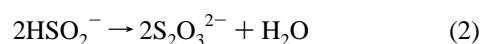
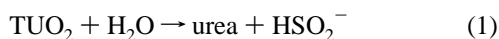


Figure 2. Time evolution of concentrations of thiourea dioxide under pH = 3.0. The decomposition reaction took place at 25.0 ± 0.1 °C with 0.04 g of TUO_2 being dissolved in 100.0 mL of water.

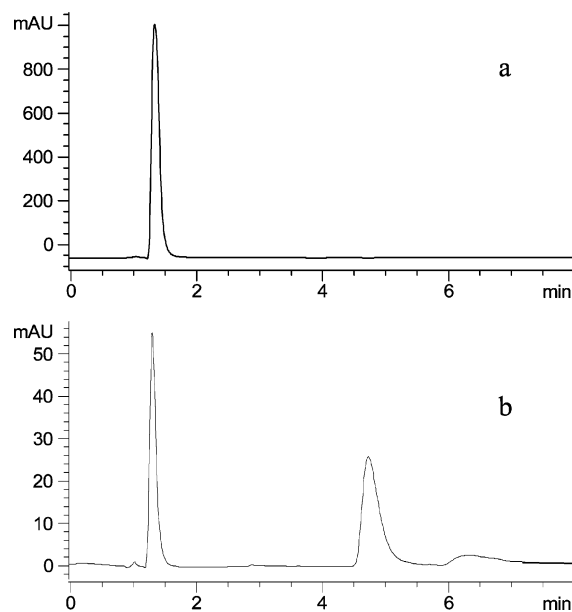


Figure 3. Chromatograms of the thiourea trioxide solution sampled at: (a) $t = 1.0$ min and (b) 9374.0 min pH of the solution is 3. The detection UV wavelength is 234.0 nm.

The concentration of thiourea dioxide is determined by comparing the area of the TUO_2 peak (at $t = 1.3$ min) with the calibrated curve (see Supporting Information), and the result is summarized in Figure 2, which illustrates how the TUO_2 concentration evolves in time at pH = 3.0. Decomposition experiments at values of pH 7.0 and 9.0 are provided in the Supporting Information. In all three cases, TUO_2 concentration decreases exponentially in time (Figure 2a). The plot of $\ln([\text{TUO}_2]_0/[\text{TUO}_2])$ vs t yields a straight line, indicating that the decomposition of thiourea dioxide is first order. Corresponding rate constants for TUO_2 decomposition are calculated, and these data are listed in Table 1.

Figure 3 characterizes the decomposition of TUO_3 in water, in which two chromatograms were collected respectively at (a) $t = 1.0$ min and (b) $t = 9374.0$ min. In this experiment 0.04 g of TUO_3 was dissolved in 100.0 mL of water and the solution

TABLE 1: Rate Constant k_1 of the Decomposition of Thiourea Dioxide and Thiourea Trioxide at Different pH Values

pH	$k_1(\text{TUO}_2)$ (s^{-1})	$k_1(\text{TUO}_3)$ (s^{-1})
3.0	7.46×10^{-7}	5.42×10^{-6}
4.0	7.73×10^{-7}	5.83×10^{-6}
5.0	8.32×10^{-7}	6.53×10^{-6}
6.0	1.67×10^{-6}	8.98×10^{-6}
7.0	6.50×10^{-5}	2.72×10^{-5}
8.0	2.56×10^{-4}	9.15×10^{-5}
9.0	3.83×10^{-4}	1.22×10^{-4}

was adjusted to pH 3.0. Because the maximum absorption wavelength of TUO₃ is around 202 nm, the detection UV wavelength used here is 220 nm. As shown in this figure, the absorption peak of TUO₃ decreased significantly after 9374.0 min, while two new peaks with the retention time of 4.6 and 6.4 min appeared in the system. Notably, the peak with a retention time of 6.4 min is observed both in the decomposition of TUO₂ and of TUO₃. It thus supports the earlier investigations which speculate that SO₃²⁻ (HSO₃⁻) is a decomposition product of TUO₂ and TUO₃.¹⁷ The following reaction (4) accounts for the formation of HSO₃⁻ from TUO₃.



We had tried to determine the nature of the species seen at $t = 4.6$ min by injecting pure urea and several similar nitrogen-containing species, but so far no match has been achieved. Again, the concentration of TUO₃ is determined by comparing the area of the TUO₃ peak ($t = 1.4$ min) with the calibration curve provided in the Supporting Information.

Figure 4a shows how the TUO₃ concentration decreases in time at pH = 3.0. Experiments under the values pH 7.0 and 9.0 are provided in the Supporting Information. In all three cases, the TUO₃ concentration decreases exponentially in time. As shown in Figure 4b, the plot of $\ln([\text{TUO}_3]_0/[\text{TUO}_3])$ vs t yields a straight line, suggesting that the decomposition of TUO₃ is first order. Corresponding rate constants for TUO₃ decomposition are calculated from the above figure, and these data can be found in Table 1. Figure 5 shows three chromatograms collected at different times during the oxidation of TUO₂ by hydrogen peroxide, in which $[\text{H}_2\text{O}_2]_0 = 2.4 \times 10^{-3}$ M, $[\text{TUO}_2]_0 = 3.0 \times 10^{-4}$ M, and the solution is pH 8.0. The detection UV wavelength used here is 234.0 nm. At the beginning of the reaction (see Figure 5a), there are only two major peaks. Separate measurements confirm that the peak at $t = 4.2$ min is due to TUO₂, whereas the peak at $t = 2.9$ min is H₂O₂. The small peak seen at $t = 3.2$ min is determined to be urea, the impurities in the TUO₂ compound. This peak was still there even after the reaction has begun for more than 50 min. The TUO₂ peak became significantly smaller in Figure 5b, indicating that the reaction has made substantial progress within the first 50 min. Remarkably, in Figure 5b a new peak appeared at $t = 4.6$ min. To determine the nature of this new compound, a small amount of TUO₃ was added to the reaction mixture, which resulted in a dramatic amplification of the peak (see Figure 5c). This HPLC analysis provides an experimental confirmation that the oxidation of TUO₂ by H₂O₂ produces TUO₃.

Figure 6a presents the time evolution of TUO₂. The initial concentration of TUO₂ was 3.0×10^{-4} M and $[\text{H}_2\text{O}_2]_0/[\text{TUO}_2]_0 = 8.0$. The reaction temperature was 25.0 ± 0.1 °C, and the reaction mixture was adjusted to pH 8.0. Under the above conditions, the reaction took longer than 60 min to complete. In Figure 6a the concentration of TUO₂ decreases exponentially

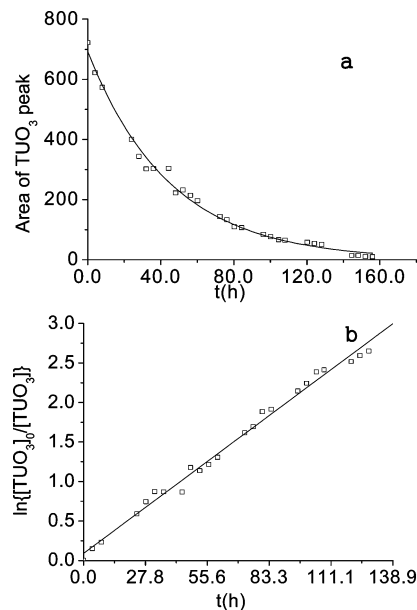


Figure 4. Time evolution of concentrations of thiourea trioxide under pH = 3. The decomposition reaction took place at 25.0 ± 0.1 °C with 0.04 g TUO₃ being dissolved in 100.0 mL water.

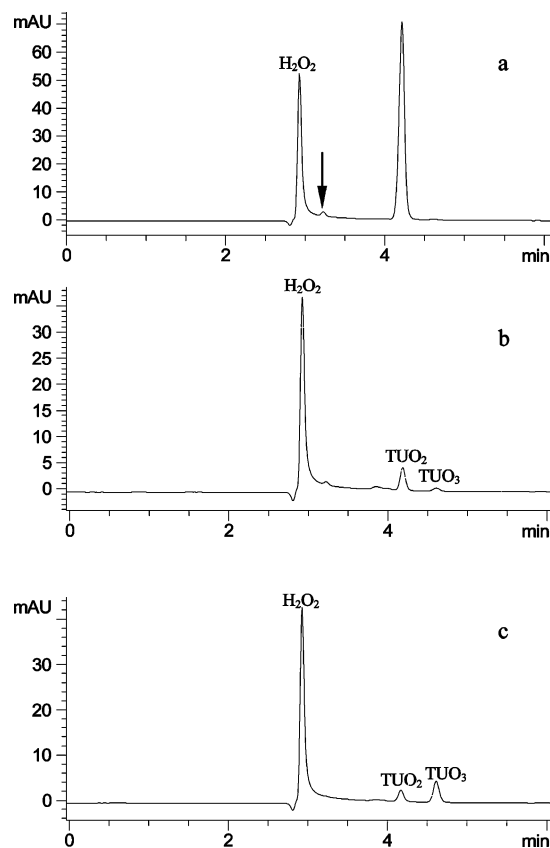


Figure 5. Chromatograms of the hydrogen peroxide–thiourea dioxide reaction collected at different times: (a) $t = 1.0$ min and (b) $t = 50.0$ min. In c, a small amount of TUO₃ is added to the reaction mixture to spike the peak seen at $t = 4.6$ min. The reaction was carried out at 25.0 ± 0.1 °C, $[\text{TUO}_2]_0 = 3.0 \times 10^{-4}$ M, $[\text{H}_2\text{O}_2]_0 = 2.4 \times 10^{-3}$ M, and pH = 8.0. The detection UV wavelength is 234.0 nm.

in time, implicating that the H₂O₂–TUO₂ reaction is first order with respect to TUO₂. It is further confirmed by plotting $\ln([\text{TUO}_2]/[\text{TUO}_2]_0)$ against t in Figure 6b, which yields a straight line. The slope of the fitted line in Figure 6b equals 8.67×10^{-4} s⁻¹. However, one must be aware that during the above

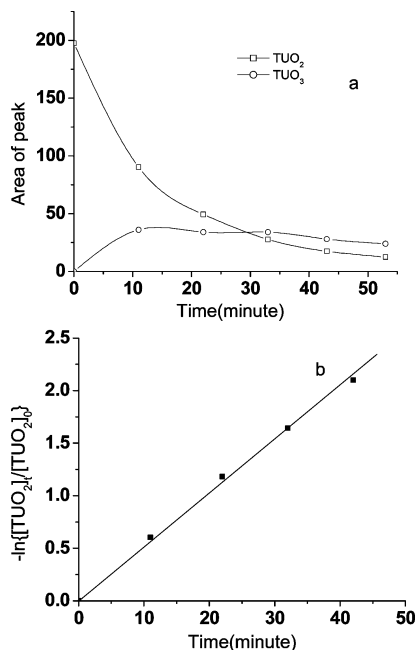
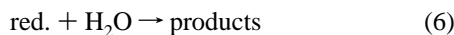


Figure 6. (a) Time evolution of concentrations of thiourea dioxide and thiourea trioxide; (b) Plot showing the variation of $\ln([TUO_2]_0/[TUO_2]_t)$ in time. The reaction was carried out at 25.0 ± 0.1 °C, $[TUO_2]_0 = 3.0 \times 10^{-4}$ M, $[H_2O_2]_0 = 2.4 \times 10^{-3}$ M, and pH = 8.0. The thiourea trioxide concentration was amplified by a factor of 20.0.

oxidation process, TUO_2 also undergoes decomposition. Therefore, strictly speaking, the reaction between thiourea oxides and H_2O_2 should be represented by the following two reactions,



where red. represents the reducing reagents TUO_2 or TUO_3 . The rate of the above reaction process should be written as

$$d[\text{red.}]/dt = -k[\text{red.}]^m[H_2O_2]^n - k_1[\text{red.}] \quad (7)$$

where k denotes the rate constant of oxidation and k_1 is the decomposition rate constant (reaction 6) obtained in the above study. A plot of $k' = (k[H_2O_2]^n + k_1)$ versus $[\text{red.}]$ in Figure 6b yields a straight line, implying that the oxidation of TUO_2 by H_2O_2 is first order with respect to TUO_2 . Through conducting a series of experiments under excessive, but different, amounts of H_2O_2 (see Figure S4 in the Supporting Information), we were able to determine that the oxidation of TUO_2 by H_2O_2 is also first order with respect to H_2O_2 . Values of k_1 and k at different pH values are listed in Table S1 of the Supporting Information.

Figure 7 presents two chromatograms collected during the H_2O_2 – TUO_3 reaction. The initial concentration of TUO_3 is 3.0×10^{-4} M and $[H_2O_2]_0/[TUO_3]_0 = 10.0$. The reaction temperature was controlled at 25.0 ± 0.1 °C, and the reaction mixture was adjusted to pH 8.0. The detection UV wavelength used is also 234.0 nm. As shown in Figure 7a, initially the mixture of TUO_3 and H_2O_2 has only two peaks in the chromatogram, which corresponds to TUO_3 ($t = 4.6$ min) and H_2O_2 ($t = 2.9$ min), respectively. The TUO_3 peak became significantly smaller in Figure 7b, which was measured at 44.0 min after mixing the two reagents together. Notably, a new peak occurred at $t = 3.2$ min, which was later confirmed as $(NH_2)_2CO$. This result provides a concrete experimental support to earlier mechanistic studies on the oxidation of TUO_3 , which suggests that oxidation products of TUO_3 are $(H_2N)_2CO$ and sulfate (see reaction 8).

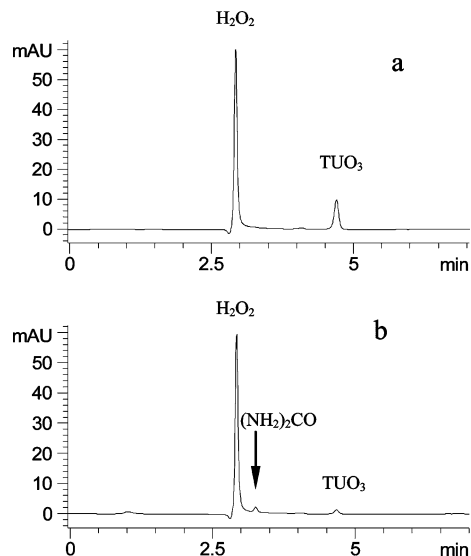


Figure 7. Chromatograms of the hydrogen peroxide–thiourea trioxide reaction collected at different times during the reaction: (a) 1.0 and (b) 44.0 min. The reaction was carried out at 25.0 ± 0.1 °C, $[TUO_3]_0 = 3.0 \times 10^{-4}$ M, $[H_2O_2]_0 = 3.0 \times 10^{-3}$ M, and pH = 8.0. The detection UV wavelength is 234.0 nm.

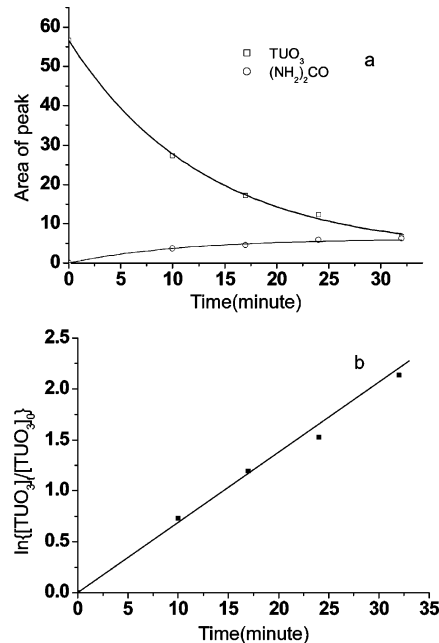


Figure 8. (a) Time evolution of concentrations of TUO_3 and $(NH_2)_2CO$. (b) Plot showing the variation of $\ln([TUO_3]_0/[TUO_3]_t)$ in time. The reaction was carried out at 25.0 ± 0.1 °C, $[TUO_3]_0 = 3.0 \times 10^{-4}$ M, $[H_2O_2]_0 = 3.0 \times 10^{-3}$ M, and pH = 8.0.

The presence of sulfate was determined by adding barium ions in acidic solution.



Time series of variations of TUO_3 and $(NH_2)_2CO$ concentrations are plotted in Figure 8. As is shown in Figure 8a, the TUO_3 concentration decreases exponentially, similar to the result obtained for the oxidation of TUO_2 (see Figure 6a). The plot of $\ln([TUO_3]_0/[TUO_3]_t)$ against t yields a straight line in Figure 8b, suggesting that the order of the reaction is 1 with respect to TUO_3 . The slope of the straight line in Figure 8b, which corresponds to k' , is calculated to be $9.53 \times 10^{-4} \text{ s}^{-1}$. A series of experiments at different H_2O_2 concentrations conducted here

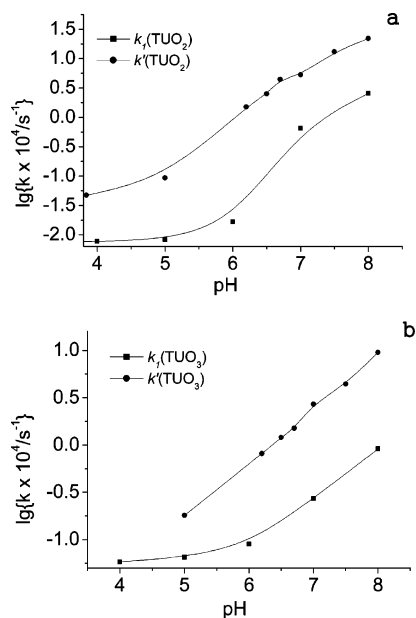


Figure 9. Dependence of rate constant k on the pH of the reaction mixture: (a) H_2O_2 – TUO_2 system, $[\text{H}_2\text{O}_2]_0 = 6.0 \times 10^{-3}$ M, and $[\text{TUO}_2]_0 = 3.0 \times 10^{-4}$ M; (b) H_2O_2 – TUO_3 system, $[\text{TUO}_3]_0 = 3.0 \times 10^{-4}$ M, and $[\text{H}_2\text{O}_2]_0 = 3.0 \times 10^{-3}$ M. Reaction temperature, $T = 25.0 \pm 0.1$ °C.

also obtained a linear relationship and second-order rate constant k by plotting k' against $[\text{H}_2\text{O}_2]$ (see Supporting Information).

To understand the influence of $[\text{H}^+]$ on the oxidation of thiourea oxides, a series of reactions have been conducted within the range between pH 4.0 and 8.0. Reaction conditions were as follows: (a) $[\text{TUO}_2]_0 = 3.0 \times 10^{-4}$ M and $[\text{H}_2\text{O}_2]_0 = 6.0 \times 10^{-3}$ M; (b) $[\text{TUO}_3]_0 = 3.0 \times 10^{-4}$ M and $[\text{H}_2\text{O}_2]_0 = 3.0 \times 10^{-3}$ M. Figure 9 plots k' as a function of pH, in which rate constants for both TUO_2 and TUO_3 are found to increase with respect to an increase of the pH of the solution (corresponding values including k' and k are provided in the Supporting Information). Such pH dependence is consistent with the result when iodine was used as the oxidant.¹⁸ To confirm that the oxidation process is the dominant part in the H_2O_2 – TUO_2 –(TUO_3) reaction, $\log k'$ (i.e., $\log(k[\text{H}_2\text{O}_2] + k_1)$) and $\log k_1$ are plotted together in Figure 9, which clearly demonstrates that the oxidation process is significantly faster than decomposition.

4. Discussion and Analysis

4.1. Effects of pH on the Decomposition and Oxidation of Thiourea Oxides. As is shown in Figure 9, increasing the pH of the solution accelerates the decomposition and oxidation of the two thiourea oxides studied here. Further examination indicates that in weakly acidic solution both the decomposition and the oxidation of TUO_3 are faster than that of TUO_2 , but the scenario becomes the opposite in alkaline solution. To understand such a transition, the relationship between the molecular structure and their reactivity needs to be considered. Thiourea oxides are known to have two structural forms:²⁰ in the solid-phase TUO_2 and TUO_3 exist as $(\text{NH}_2)_2\text{CSO}_2$ and $(\text{NH}_2)_2\text{CSO}_3$, respectively, yet they tautomerize to acidic forms $\text{H}_2\text{N}(\text{NH})\text{CSO}_2\text{H}$ and $\text{NH}_2(\text{NH})\text{CSO}_3\text{H}$ in aqueous solution. The decomposition and oxidation of thiourea oxides arise from the attack of H_2O (or OH^-) molecules and oxidants such as hydrogen peroxide on the carbon and sulfur atoms. Clearly, the rates of these processes depend on the positive electricity of carbon and sulfur atoms as well as their spatial conformation. More specifically, nucleophilic attack from the solvent and

oxidants could be strengthened by the positive charge on carbon and sulfur atoms, but would be blocked by the sulfur–oxygen group.

As to the pH effects, increasing the pH of the aqueous solution results in more and more deprotonated molecules of thiourea oxides and therefore accelerates their decomposition and oxidation. The deprotonation constant $\text{p}K_a$ of TUO_3 is smaller than that of TUO_2 ($\text{p}K_a = 8.01$).²¹ In the acidic solution, therefore, there is a higher percentage of deprotonated TUO_3 than that of TUO_2 , which consequently causes more positive charges on the carbon and sulfur atoms. As a result, TUO_3 becomes more susceptible to nucleophilic attack in acidic environment than TUO_2 (i.e., the decomposition and oxidation of TUO_3 become faster than that of TUO_2). In the alkaline solution, both TUO_2 and TUO_3 are largely deprotonated, in which the conformation of the sulfur–oxygen group plays the main role in limiting nucleophilic attack on carbon and sulfur atoms. Obviously the SO_3^- group is larger than the SO_2^- group. In addition, the geometry around the sulfur atom in TUO_2 is planar, whereas it is tetrahedral in TUO_3 . The smaller SO_2^- group blocks the attacking weakly and consequently makes the reactivity of TUO_2 stronger than that of TUO_3 .

4.2. New Mechanistic Insights from the Direct Identification of Different Components. During the decomposition and oxidation of thiourea oxides by H_2O_2 , multiple components were followed simultaneously by HPLC. For example, HPLC could quantify H_2O_2 , urea, TUO_2 , and TUO_3 . During the oxidation of TUO_2 , the concentration of TUO_3 is found to rise first and then decrease. Such a scenario suggests that the most probable oxidation path of TUO_2 is through the production of TUO_3 and then TUO_3 is oxidized to SO_4^{2-} . When the pH is smaller than pH 8.0, the decomposition of TUO_2 could be negligible.

According to previous works,¹⁷ the oxidation process of TUO_2 in strong alkaline solution consists of decomposition and oxidation steps. Thiourea oxides decompose to dioxosulfate (SO_2^{2-}), and then SO_2^{2-} is further oxidized. This study illustrates that depending on pH values, the oxidation reaction may be carried by different mechanisms. For example, Figure 9a shows that $(k[\text{H}_2\text{O}_2] + k_1)/k_1$ is mostly larger than 10, implying that the nucleophilic attack on sulfur atom is the dominant reaction under the condition smaller than pH 8.0. Figure 9b indicates that the oxidation of TUO_3 by H_2O_2 is similar to the oxidation of TUO_2 but is somehow different from their oxidations by iodine,¹⁸ which were found to be zero-order in iodine within the studied range of pH 2–6. Presumably, the difference arises from the fact that iodine is a weak nucleophilic oxidant as well as its relatively bigger size. This study therefore suggests that the stability and reactivity of the two thiourea oxides are decided not only by their molecular structure and pH conditions but also by properties of oxidant.

5. Summary

A reverse-phase ion-pair high-performance liquid chromatography method was employed here to investigate the decomposition and oxidation kinetics of thiourea oxides. Our experiments show that multiple sulfur-containing species including TUO_2 , TUO_3 , sulfite, and $(\text{NH}_2)_2\text{CO}$ could be determined and quantified simultaneously. These experiments illustrate that the oxidation of TUO_2 and TUO_3 is first order with respect to the reducing reagents (i.e., thiourea oxides). Such a result is consistent with the oxidations by other oxidants.¹⁸ In addition, the oxidation of TUO_2 and TUO_3 also appears to be first order with respect to the oxidant H_2O_2 .

When the pH of the solution is increased, the decomposition and oxidation of thiourea oxides also become faster. Moreover,

in weakly acidic solution the decomposition and oxidation of TUO₃ have larger reaction rates than those of TUO₂, but in alkaline solution the result is reversed. The above phenomena are attributed to the conformation and charge effects for nucleophilic attacking on carbon and sulfur atoms. The mechanism of the oxidation of thiourea oxides appears to depend on their structure, the pH of the solution, and the oxidant. Using hydrogen peroxide as the oxidant, in strong alkaline medium decomposition of thiourea oxides is the rate-determining step. In neutral and acidic solutions, oxidation takes place through the direct attack on the sulfur atom by the oxidant. This new insight could be particularly useful for probing the mechanism of nonlinear phenomena involved in oxidation of sulfur species and manipulating product compositions of the oxidation of thiourea and its oxides.²⁰

Acknowledgment. We gratefully acknowledge the fruitful discussion with Prof. Sergei Makarov during his visit to CUMT. This work is supported through RFDP (Grant 20050290512), NSFC (Grant 20573134), and NCET (Grant 05-0477) of China. J.W. thanks CUMT for a visiting professor fellowship.

Supporting Information Available: Plots showing the linear relationship between the standard concentration and the integrated area of peaks in the chromatogram, the time evolution of concentrations of thiourea dioxide under different pH conditions, the time evolution of concentrations of TUO₃ under different pH conditions, a plot of the apparent rate constant k' 's vs H₂O₂ concentration in the H₂O₂-TUO₂ system, and the table of pseudo-first order and second order rate constants in the oxidation of thiourea oxides at different pH values by hydrogen

peroxide. This material is available free of charge via the Internet at <http://pubs.acs.org>.

References and Notes

- (1) Jonnalagadda, S. B.; Chinake, C. R.; Simoyi, R. H. *J. Phys. Chem.* **1996**, *100*, 13521.
- (2) Simoyi, R. H.; Epstein, I. R. *J. Phys. Chem.* **1987**, *91*, 5124.
- (3) Chinake, C. R.; Simoyi, R. H. *J. Phys. Chem.* **1993**, *97*, 11569.
- (4) Maryanoff, C. A.; Stanzione, R. C.; Plampin, J. N. *Phosphorus Sulfur Relat. Elem.* **1986**, *27*, 221.
- (5) Dempsey, R. O.; Browne, K. A.; Bruce, T. C. *J. Am. Chem. Soc.* **1995**, *117*, 6140.
- (6) Mantri, P.; Duffy, D. E.; Kettner, C. A. *J. Org. Chem.* **1996**, *61*, 5690.
- (7) Kim, K.; Lin, Y. T.; Mosher, H. S. *Tetrahedron Lett.* **1988**, *29*, 3183.
- (8) Maryanoff, C. A.; Stanzione, R. C.; Plampin, J. N.; Mills, J. E. *J. Org. Chem.* **1986**, *51*, 1882.
- (9) Abou-Zeid, N. Y.; Waly, A.; Higazy, A.; Hebeish, A. *Angew. Makromol. Chem.* **1986**, *143*, 85.
- (10) Borgogno, G.; Colonna, S.; Fornasier, R. *Synthesis* **1975**, *8*, 529.
- (11) Drabowicz, S.; Mikolajczyk, M. *Synthesis* **1978**, *7*, 542.
- (12) Makarov, S. V.; Mundoma, C.; Penn, J. H.; Svarovsky, S. A.; Simoyi, R. H. *J. Phys. Chem. A* **1998**, *102*, 6786.
- (13) Alamgir, M.; Epstein, I. R. *Int. J. Chem. Kinet.* **1985**, *17*, 429.
- (14) Simoyi, R. H. *J. Phys. Chem.* **1987**, *91*, 2802.
- (15) Doona, C. J.; Blittersdorf, R.; Schneider, F. W. *J. Phys. Chem.* **1993**, *97*, 7258.
- (16) Xu, L.; Gao, Q.; Feng, J.; Wang, J. *Chem. Phys. Lett.* **2004**, *397*, 265.
- (17) Svarovsky, S. A.; Simoyi, R. H.; Makarov, S. V. *J. Phys. Chem. B* **2001**, *105*, 12634.
- (18) Makarov, S. V.; Mundoma, C.; Penn, J. H.; Petersen, J. L.; Svarovsky, S. A.; Simoyi, R. H. *Inorg. Chim. Acta* **1999**, *286*, 149.
- (19) Grigorova, R.; Wright, S. A. *J. Chromatogr.* **1986**, *368*, 444.
- (20) Makarov, S. V. *Russ. Chem. Rev.* **2001**, *20*, 885.
- (21) Svarovsky, S. A.; Simoyi, R. H.; Makarov, S. V. *J. Chem. Soc., Dalton Trans.* **2000**, 511.